RESEARCH ARTICLE

Factors Required for Activation of Urease as a Virulence Determinant in *Cryptococcus neoformans*

Arpita Singh,[a] Robert J. Panting,[b]* Ashok Varma,[a] Tomomi Saijo,[a] Kevin J. Waldron,[b] Ambrose Jong,[c] Popchai Ngamskulrungroj,[a,d]* Yun C. Chang,[a] Julian C. Rutherford,[b] Kyung J. Kwon-Chung[a]

Molecular Microbiology Section, Laboratory of Clinical Infectious Diseases, National Institute of Allergy and Infectious Diseases, NIH, Bethesda, Maryland, USA[a]; Institute for Cell and Molecular Biosciences, Medical School, Newcastle University, Newcastle upon Tyne, United Kingdom[b]; Division of Hematology-Oncology, Saban Research Institute, Children's Hospital Los Angeles, Keck School of Medicine, University of Southern California, Los Angeles, California, USA[c]; Department of Microbiology, Mahidol University, Bangkok, Thailand[d]

A.S., R.J.P., and A.V. contributed equally to this article.

* Present address: Robert J. Panting, Fujifilm Diosynth Biotechnologies, Billingham, United Kingdom; Popchai Ngamskulrungroj, Department of Microbiology, Mahidol University, Bangkok, Thailand.

ABSTRACT **Urease in *Cryptococcus neoformans* plays an important role in fungal dissemination to the brain and causing meningoencephalitis. Although urea is not required for synthesis of apourease encoded by *URE1*, the available nitrogen source affected the expression of *URE1* as well as the level of the enzyme activity. Activation of the apoenzyme requires three accessory proteins, Ure4, Ure6, and Ure7, which are homologs of the bacterial urease accessory proteins UreD, UreF, and UreG, respectively. A yeast two-hybrid assay showed positive interaction of Ure1 with the three accessory proteins encoded by *URE4*, *URE6*, and *URE7*. Metalloproteomic analysis of cryptococcal lysates using inductively coupled plasma mass spectrometry (ICP-MS) and a biochemical assay of urease activity showed that, as in many other organisms, urease is a metallocentric enzyme that requires nickel transported by Nic1 for its catalytic activity. The Ure7 accessory protein (bacterial UreG homolog) binds nickel likely via its conserved histidine-rich domain and appears to be responsible for the incorporation of Ni^{2+} into the apourease. Although the cryptococcal genome lacks the bacterial UreE homolog, Ure7 appears to combine the functions of bacterial UreE and UreG, thus making this pathogen more similar to that seen with the plant system. Brain invasion by the *ure1*, *ure7*, and *nic1* mutant strains that lack urease activity was significantly less effective in a mouse model. This indicated that an activated urease and not the Ure1 protein was responsible for enhancement of brain invasion and that the factors required for urease activation in *C. neoformans* resemble those of plants more than those of bacteria.**

IMPORTANCE ***Cryptococcus neoformans* is the major fungal agent of meningoencephalitis in humans. Although urease is an important factor for cryptococcal brain invasion, the enzyme activation system has not been studied. We show that urease is a nickel-requiring enzyme whose activity level is influenced by the type of available nitrogen source. *C. neoformans* contains all the bacterial urease accessory protein homologs and nickel transporters except UreE, a nickel chaperone. Cryptococcal Ure7 (a homolog of UreG) apparently functions as both the bacterial UreG and UreE in activating the Ure1 apoenzyme. The cryptococcal urease accessory proteins Ure4, Ure6, and Ure7 interacted with Ure1 in a yeast two-hybrid assay, and deletion of any one of these not only inactivated the enzyme but also reduced the efficacy of brain invasion. This is the first study showing a holistic picture of urease in fungi, clarifying that urease activity, and not Ure1 protein, contributes to pathogenesis in *C. neoformans***

Received 27 March 2013 **Accepted** 2 April 2013 **Published** 7 May 2013

Citation Singh A, Panting RJ, Varma A, Saijo T, Waldron KJ, Jong A, Ngamskulrungroj P, Chang YC, Rutherford JC, Kwon-Chung KJ. 2013. Factors required for activation of urease as a virulence determinant in *Cryptococcus neoformans*. mBio 4(3):e00220-13. doi:10.1128/mBio.00220-13.

Editor Joseph Heitman, Duke University

Address correspondence to Julian C. Rutherford, Julian.Rutherford@newcastle.ac.uk, or Kyung J.Kwon-Chung, june_kwon-chung@nih.gov.

One of the hallmarks that differentiate *Cryptococcus neoformans* from other white clinical yeasts is its ability to produce urease. Urease-negative *C. neoformans* strains have rarely been isolated from patients or the environment (1), and the enzyme is recognized as an important virulence factor in *C. neoformans* and in other fungal pathogens that initiate infection in the lungs (2–4). The genetics and biochemistry of the urease system have been extensively studied in bacteria (5) and plants (6–8) but not in fungi. Although urease has been identified in few fungal species (9, 10) and was purified and crystallized from *Coccidioides immitis* (11), the machinery involved in its activation has not been characterized.

Urease from Jack bean was the first enzyme to be crystallized over 80 years ago (12). Crystallographic analysis of urease in bacteria revealed that it is comprised of three polypeptides encoded by the genes *ureA*, *ureB*, and *ureC*. These form a trimer $(UreA\text{-}UreB\text{-}UreC)_3$ that contains a binuclear nickel (Ni) metallocenter per UreC (13, 14). Activation of the urease apoenzyme by binding

Ni *in vivo* requires four accessory proteins, *viz*., UreD, UreE, UreF, and UreG (15, 16). Plant ureases resemble bacterial ureases in both sequence and structure. However, while bacterial ureases are multimers of two or three polypeptide chains, plant ureases consist of a single 90-kDa polypeptide chain formed by fusion of trimeric subunits in a collinear fashion that requires activation by the three accessory proteins UreD, UreF, and UreG. In plants (17) and fungi, the homolog of UreE protein has not yet been identified.

In *C. neoformans*, the *URE1* gene (CNAG_05540) encodes the urease apoenzyme, which has been deleted and studied for its role in virulence (2, 18). However, the role of an activated urease versus the Ure1 protein in virulence is yet to be clarified. In addition, *URE2*, which has no known function and was found to functionally complement the urease-negative clinical strain B-4587 (1), is an enigma since the gene is a homolog of the chromosome segregation-associated proteins (19) such as Smc3 of *Arabidopsis thaliana* and SudA of *Aspergillus nidulans* (20). In similarity to the urease system in other organisms, the *C. neoformans* genome contains *NIC1*, which encodes a nickel transporter, and the accessory protein genes *URE4*, *URE6*, and *URE7*, which are homologs of the bacterial *ureD*, *ureF*, and *ureG* genes, respectively. The bacterial gene encoding a homolog of the nickel chaperone protein UreE, however, is absent in the *C. neoformans* genome. Absence of the UreE homolog in *C. neoformans* suggests an as-yet-unidentified alternative mechanism by which Ni might be delivered to the urease apoenzyme complex.

This study had the following objectives: (i) to uncover the function(s) of the accessory proteins and determine their association with the Ure1 protein; (ii) to clarify the role of *URE2*; and (iii) to determine the effect of urease activity versus Ure1 protein in brain invasion. We found that the *URE1* expression level is affected by the nitrogen source and that all three accessory proteins are essential for urease activity in *C. neoformans*. *NIC1* encodes a nickel permease, and the Ure7 protein serves as the Ni carrier with a combined role of bacterial proteins UreE and UreG. Each of the accessory proteins Ure4, Ure6, and Ure7 interacted with the Ure1 protein. The *URE2* gene was found to be unrelated to the urease system. It was apparently mistaken for the *URE4* function during complementation attempts due to the tight linkage between the two genes on the DNA insertion used for complementation. Importantly, it was found to be urease activity and not Ure1 protein that assists in the cryptococcal brain invasion by affecting the integrity of the brain microvascular endothelial cell (BMEC) membrane.

RESULTS

The type of available nitrogen source regulates the level of *URE1* expression and the enzyme activity. To identify the effect of different nitrogen sources in growth media that may influence cryptococcal urease activity, wild-type H99 (WT) cells were grown in various nitrogen sources. While *URE1* transcripts were observed in cells grown in urea-free media supplemented with ammonium or proline as the sole nitrogen source, the transcripts were clearly more abundant in urea-grown cells (Fig. 1A, inset). This was further corroborated by measurements of urease activity. Cells grown in urea exhibited much higher levels of urease activity than cells grown in yeast extract-peptone-dextrose (YPD) (Fig. 1A). Urease activity in ammonium-grown cells was approximately 60% of activity seen with the urea-grown cells, while intermediate levels were observed in proline-, glutamine-, and glutamic acid-grown cells. Therefore, cryptococcal *URE1* expression and the enzyme activity are regulated in response to the available nitrogen source.

The accessory proteins Ure4, Ure6, and Ure7 are essential for cryptococcal urease activity. Each of the three genes homologous to the bacterial urease accessory protein genes was deleted in the *C. neoformans* H99 strain. All the urease accessory protein mutants, *viz*., mutants *ure4*Δ, *ure6*Δ, and *ure7*Δ, failed to grow on agar media with urea as the sole nitrogen source (Fig. 1B, upper panel) and showed no color development on Christensen's urea media at both early (24 h) and late (48 h) (Fig. 1B, lower panel) time points. All the corresponding reconstituted strains, *viz*., strains *ure4*Δ+*URE4*, *ure6*Δ+*URE6*, and *ure7*Δ+*URE7*, grew well and developed color comparable to that seen with the H99 strain at both time points. These results indicated that each of the urease accessory proteins is essential for urease enzyme function.

To further validate this result, urease activity was assayed in cell lysates prepared from each of the urease accessory protein mutant strains. Urease activity in the WT cells was recorded as 675 ± 158 U/g while the enzyme activity was undetectable in the *ure4*Δ, *ure6*Δ, and *ure7*Δ strains, as was the case with the *ure1*Δ strain (Fig. 1C). These findings demonstrate that the Ure4, Ure6, and Ure7 proteins are functionally homologous to the bacterial urease accessory proteins and are required for urease activity.

Cryptococcal urease is a nickel enzyme such as is found in other organisms. To identify the metal cofactor of cryptococcal urease, the metal profile and enzyme activity in soluble cell extracts from the WT strain were determined. Extracts were prepared and fractionated under anaerobic (<2 ppm O_2) and nondenaturing conditions using a combination of anion exchange and size exclusion high-performance liquid chromatography (HPLC). This method ensures the coelution of metalloproteins with their respective metal ions to reflect *in vivo* protein-metal associations (21, 22). Urease activity and metal levels were quantified using a standard enzyme assay and inductively coupled plasma mass spectrometry (ICP-MS), respectively. Urease activity was detected in the high-molecular-weight fractions from the WT strain but was absent in the equivalent fractions from the *ure1*Δ strain (Fig. 2A). ICP-MS elemental analysis demonstrated the presence of nickel within these urease-positive fractions from WT extracts that was lacking in the equivalent fractions from the *ure1*Δ strain (Fig. 2B). Interestingly, the elution characteristics of a low-molecular-weight nickel pool increased in the mutant strain, which could have been due to the association of Ni with a low-molecular-weight ligand, possibly for vacuolar storage (23, 24). Quantification of other metal ions established that only nickel coeluted with the urease activity (data not shown). The coelution of nickel in wild-type fractions with urease activity, which was absent in the *ure1*Δ strain, indirectly establishes an *in vivo* association of nickel with the cryptococcal urease enzyme.

Ure7 supplies nickel for the functional urease. The *C. neoformans* genome contains an open reading frame (CNAG_00678.2) that codes for a protein homologous to the bacterial UreG urease accessory protein. This (cryptococcal Ure7) protein contains sequences that are found to be conserved within the Ras-like superfamily of small guanosine triphosphatases such as the GTP binding P-loop in the amino-terminal region (residues 115 to 122) and switch domains that undergo a conformational change upon GTP binding (residues 147 to 154 and 171 to 172) (see Fig. S1A in the supplemental material). In contrast to most of the bacterial UreG

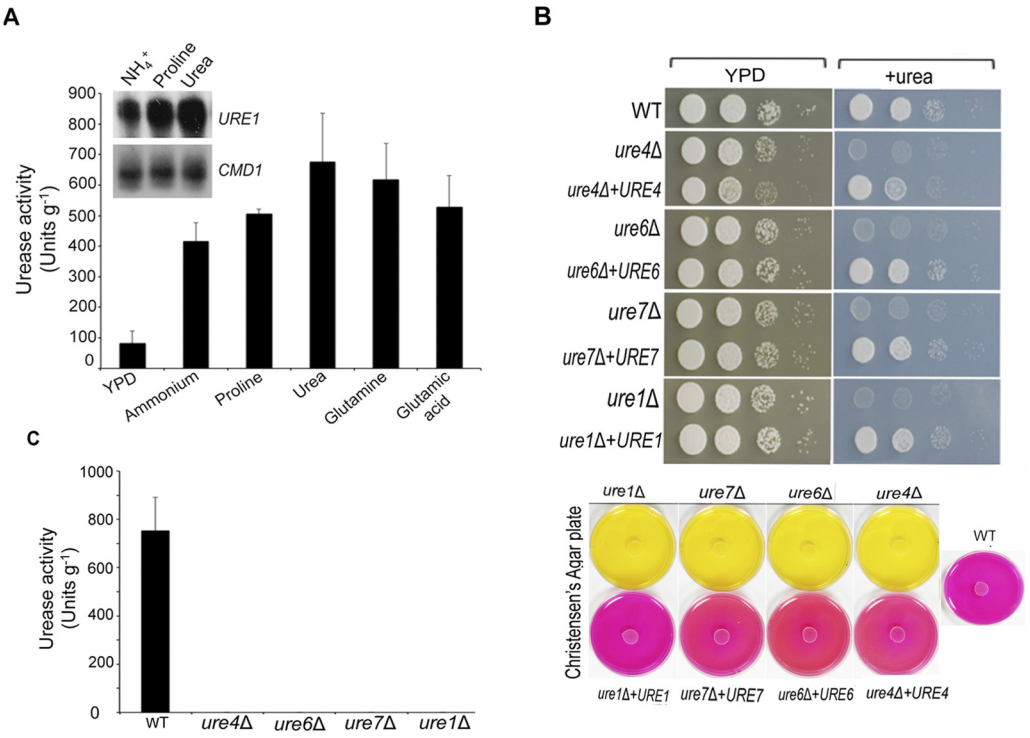

FIG 1 Regulation of *URE1* expression and urease activity by different nitrogen sources and the requirement of accessory proteins Ure4, Ure6, and Ure7 for urease activity. (A) The *URE1* transcript level is regulated in response to the nitrogen source (figure inset). The level of calmodulin transcript (*CMD1*) was used as a loading control. Urease activity was quantified in cells grown in rich YPD or YNB medium with ammonium, proline, urea, glutamine, or glutamic acid as the sole nitrogen source. Cells grown in YNB with urea as the sole nitrogen source showed the highest activity. (B) Upper panel: a spot assay for growth of the WT, accessory protein mutant and complemented strains on YPD and YNB agar media supplemented with urea as the only nitrogen source after 48 h of incubation. Lower panel: a spot assay for all the urease accessory protein mutants on Christensen's urea agar. Absence of the magenta color indicates the loss of urease activity. (C) Biochemical assay of urease activity in the cell extracts from the WT, *ure4*Δ, *ure6*Δ, *ure7*Δ, and *ure1*Δ strains.

proteins, Ure7 has 17 histidine residues over a stretch of 52 amino acids at its amino-terminal end (see Fig. S1A in the supplemental material). *C. neoformans* lacks a homolog of the UreE bacterial nickel chaperone, but histidine residues are potential nickel binding sites (25, 26), which suggested that the Ure7 amino-terminal domain might also function as a nickel chaperone.

To analyze the role of Ure7, urease and nickel profiles of the Ure7-deficient strain (*ure7*Δ) and its complemented strain (*ure7*Δ+*URE7*) were determined in the same way as was done in the WT strain (Fig. 2A and B). Quantification of urease activity identified those fractions from the *ure7*Δ+*URE7* strain that contained enzyme activity (Fig. 2C). No urease activity was identified in the equivalent fractions from the *ure7*Δ strain. Analysis of nickel levels established that the *URE7*-complemented strain contained the nickel pools previously identified in WT cells (Fig. 2B and D). In similarity to the wild-type nickel profile (Fig. 2B), the high-molecular-weight nickel pool was detected only in those fractions that contained urease activity in the *ure7*Δ+*URE7* strain (Fig. 2D). In contrast, the urease-associated nickel pool was absent in extracts from the *ure7*Δ strain. The finding of similar nickel profiles of a mutant lacking Ure7 (*ure7*Δ) and of the *ure1*Δ mutant therefore supports a model where cryptococcal Ure7 is required for the acquisition of nickel by the urease apoenzyme *in vivo*.

To determine the nickel binding characteristics of Ure7 *in vitro*, the protein was isolated from a bacterial expression system. The purified protein was confirmed to be Ure7 by matrix-assisted laser desorption ionization (MALDI)-peptide mass fingerprinting (27) (data not shown). Initial analysis of the metal content by ICP-MS identified substoichiometric quantities of nickel associated with recombinant Ure7 following its purification from *Escherichia coli*. As an initial determination of nickel binding to Ure7, the UV-visible light spectrum of Ure7 was monitored as up to 5 M equivalents (Eq) of nickel were added (Fig. 2E). The difference spectra resulting from the subtraction of the apo spectrum from the nickel-protein spectra revealed a new band at 326 nm when more than 2 Eq of nickel was added. This band is consistent with a ligand-to-metal charge transfer (LMCT), which is diagnostic of nickel binding to UreG (28). The addition of higher levels of nickel was not possible due to protein precipitation.

The identified LMCT transitions may reflect a mixture of high-affinity nickel binding sites and metal more loosely associated with Ure7. Two approaches were undertaken to determine the stoichiometry of nickel binding to Ure7. First, a solution of Ure7 was incubated with an excess of nickel and the loosely associated nickel was removed by filtration through a Sephadex G-25 desalting column. Quantification of the amount of metal associated with the protein by ICP-MS showed that two nickel atoms associate with each Ure7 monomer (1.94 ± 0.21 [means ± standard deviations {SD}]). To further analyze the stoichiometry of nickel binding to Ure7, equilibrium dialysis was performed. Apo-Ure7 was dialyzed against increasing concentrations of nickel and the final number of atoms per Ure7 monomer determined by ICP-MS. The binding

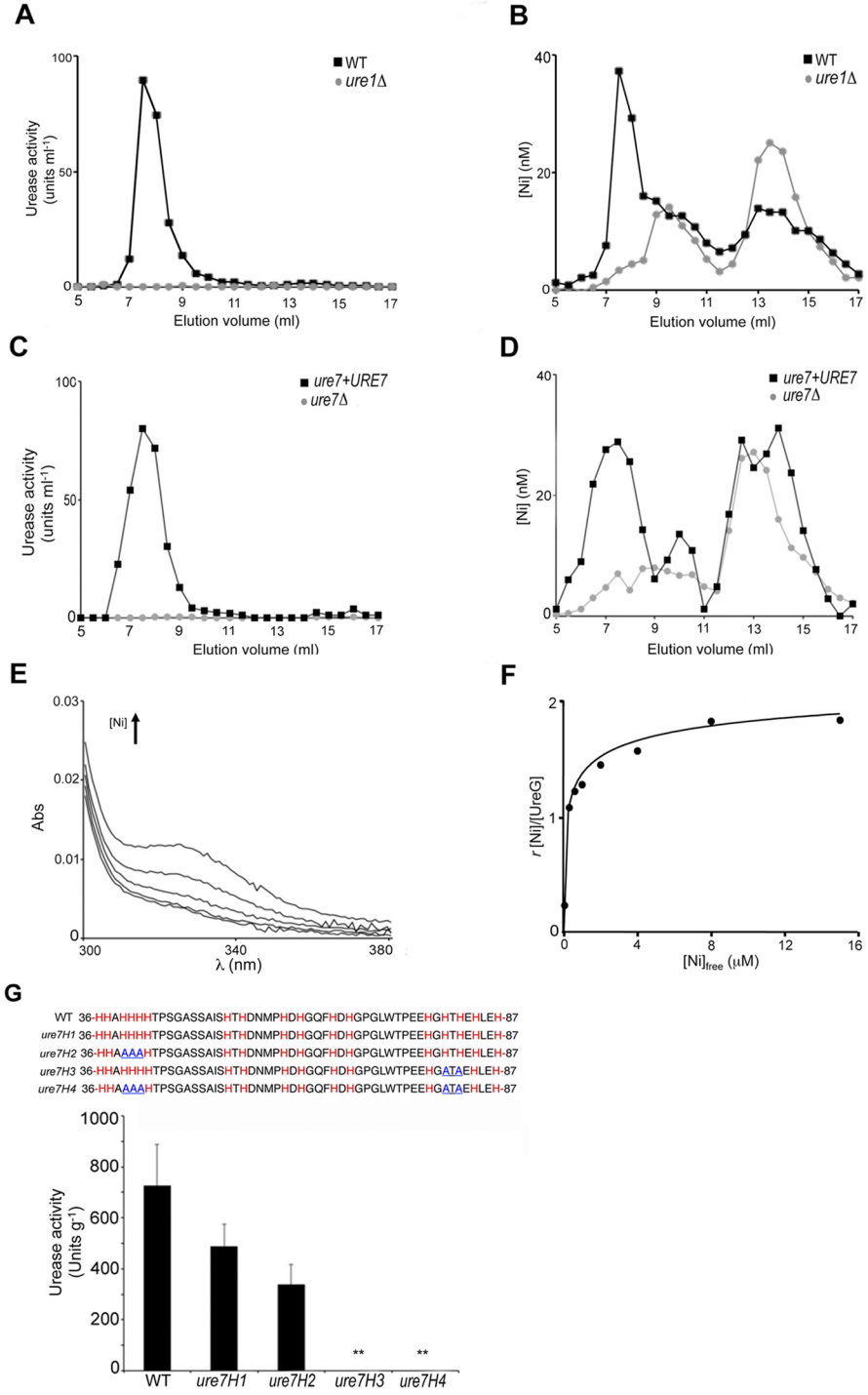

FIG 2 Cryptococcal urease is a nickel enzyme, and the conserved His-rich domain of Ure7 is required for urease activity. (A and B) Soluble extracts from WT and the *ure1*Δ strain grown in glutamic acid medium were fractionated. Urease activity (A) and nickel content (B) were quantified in each fraction eluted from the ion exchange column with 300 mM sodium chloride. Nickel pools were observed in the urease-positive WT strain and not in the identical fractions from the *ure1*Δ strain. (C and D) Soluble extracts from the *ure7*Δ strain and the complemented *URE7* strain (*ure7*Δ+ *URE7*) were fractionated and urease activity (C) and nickel levels (D) quantified in each fraction. Data are shown for those fractions eluted from the ion exchange column with 300 mM sodium chloride. (E) Difference UV-visible light absorption spectra of Ure7 generated by subtracting the apo spectrum from the nickel-protein spectra following the addition of 1 to 5 M equivalents of nickel, showing that Ure7 binds nickel *in vitro*. (F) Stoichiometry of nickel binding to Ure7 determined by equilibrium dialysis. Apo-Ure7 was dialyzed overnight against increasing concentrations of nickel and the level of protein-associated nickel determined by ICP-MS. (G) The upper panel shows the region with conserved His-rich sites of Ure7. The histidines are marked in red, while the substituted alanines are marked in blue. Urease activity assays for all the *ure7H* mutants containing a mutated His site. The *ure7H3* mutant with an alanine substitution at His-rich residues 80 to 82 and the *ure7H4* mutant with a substitution at both residues 39 to 41 and residues 80 to 82 showed a complete absence of urease activity. **, $P < 0.001$ (compared to the *ure7H1* mutant results).

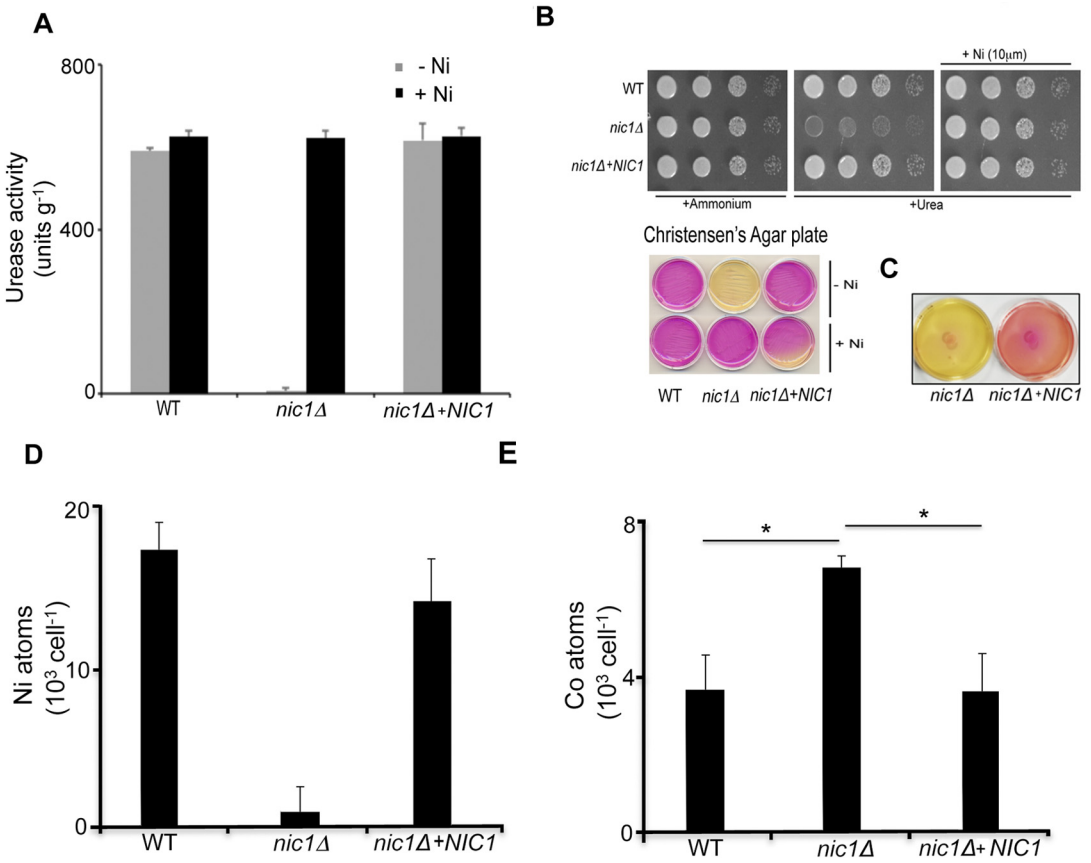

FIG 3 Nic1 is required for urease activity in *C. neoformans*. (A) WT, *nic1*Δ, and *nic1*Δ+*NIC1* strains were grown in synthetic glutamic acid medium, with (black bars) and without (gray bars) supplemented nickel (10 μM), and urease activity was quantified using Nessler's reagent. (B) A suspension of WT, *nic1*Δ, and *nic1*Δ+*NIC1* strains, grown overnight in ammonium medium, was spotted onto ammonium, urea, and Christensen's agar plates with and without added nickel (10 μM) at 30°C. (C) A spot assay on Christensen's urea agar after 48 h of incubation shows that the *NIC1* deletant strain (*nic1*Δ) became slightly urease positive in a delayed manner. (D and E) Nic1 is required for nickel accumulation (D) but not cobalt accumulation (E). Nickel and cobalt levels were quantified by ICP-MS in WT, *nic1*Δ, and *nic1*Δ+*NIC1* strains that had been grown in synthetic media containing glutamic acid as the sole nitrogen source. *, $P < 0.05$ (compared to the *nic1*Δ strain).

of nickel to Ure7 reached saturation at 2.18 ± 0.21 (means ± SD) metal ions per monomer of protein with a calculated dissociation constant (K_d) of less than 1 μM (Fig. 2F). Thus, Ure7 can bind nickel and may function as a nickel chaperone.

Histidine residues are potential nickel binding sites. There are two highly conserved His-rich domains among fungal and plant UreG proteins (see Fig. S1B in the supplemental material). To analyze the importance of these domains in Ure7 of the cryptococcal urease system, several histidine residues at amino acids (aa) 39 to 41 and/or aa 80 to 82 of the sequence of Ure7 were replaced with alanine (Fig. 2G, upper panel). The urease activity of the resulting mutants was analyzed. The urease activity in the *ure7H3* and *ure7H4* mutants was abolished completely, while in the *ure7H2* strain it was close to that of the control wild-type construct *ure7H1* (Fig. 2G, P = 0.13). Furthermore, growth of the *ure7H3* and *ure7H4* mutants was greatly retarded in media containing urea as the sole nitrogen source (data not shown). Thus, histidine residues between aa 80 and 82 of Ure7 appear to facilitate nickel binding for the cryptococcal functional urease.

Nic1 is a Ni permease required for urease activity. The *C. neoformans* genome contains a gene (CNAG_03664.2) encoding a protein homologous to the family of nickel and cobalt transporter proteins, which include *HoxN* in *Cupriavidus metallidurans* and *Nic1* in *Schizosaccharomyces pombe* (29–32). Based on the described homology to known nickel transporters, we designated the cryptococcal HoxN/Nic1 homolog Nic1.

To determine if Nic1 is required for urease activity, the WT, the *nic1*Δ, and the *nic1*Δ+*NIC1* strains were grown in glutamic acid medium. Urease activity was undetectable in extracts from the *nic1*Δ strain unless the growth medium was supplemented with 10 μM nickel (Fig. 3A). Consistent with these results were the plate assays of growth in urea medium and the ability of these three strains to turn Christensen's medium pink (Fig. 3B). However, longer incubation of the *nic1*Δ strain in Christensen's agar produced a light pink color (Fig. 3C), suggesting the possible presence of another transporter(s) with lower Ni affinity in addition to Nic1.

Analysis of cellular metal content by ICP-MS identified a lack of nickel accumulation in the *nic1*Δ strain when grown with glutamic acid as the sole nitrogen source (Fig. 3D). These data are consistent with Nic1 being a nickel transporter required for urease activity in *C. neoformans*. To determine if Nic1 is specific for nickel, the cellular cobalt content was also quantified in the three strains. Levels of accumulated cobalt were high in all three strains

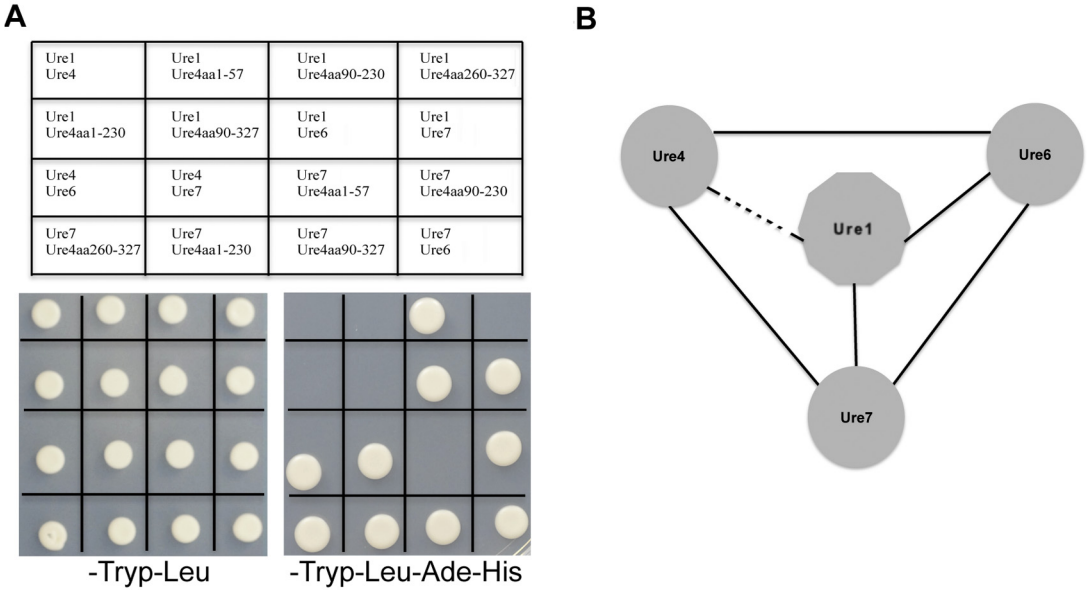

FIG 4 Yeast two-hybrid assays identify the interaction of Ure1 with its accessory proteins. (A) Transformants were spotted as marked in the grid (upper panel). The results of spot assays of the yeast two-hybrid interaction on control SD-Trp-Leu medium (lower left panel) and selective SD-Trp-Leu-His-Ade medium (lower right panel) are shown. Growth on the selective medium implies a positive interaction between the proteins. (B) Schematic representation of the interaction between Ure1 and the accessory proteins in yeast two-hybrid assays. The dotted line represents a very weak or no interaction between Ure1 and Ure4.

when grown in glutamic acid medium, with the *nic1*Δ strain accumulating more than wild-type levels of cobalt (Fig. 3E), suggesting that *C. neoformans* Nic1 is a nickel-specific transporter.

Cryptococcal urease accessory proteins interact with the urease apoenzyme. To determine a role for the Ure4, Ure6, and Ure7 accessory proteins in activation of the urease apoenzyme in *C. neoformans*, the yeast two-hybrid (Y2H) assay was used. We systematically studied pairwise interactions where a single "bait" test protein was individually assayed in a Y2H system against a "prey" test protein (33, 34). An interaction was measured as a function of growth on selective media (quadruple-drop-out [QDO] media without tryptophan, leucine, adenine, and histidine) (Fig. 4A, lower panel) and confirmed by growth and color development on high-stringency selective media (QDO media supplemented with the drug aureobasisin A and 5-bromo-4-chloro-3-indolyl-α-D-galactopyranoside [X-α-Gal]; data not shown). Initially, Ure1 failed to show any interaction with the full-length Ure4 protein. Thus, the probability of the presence of transmembrane domain helices in this protein (http://www.cbs.dtu.dk/services/TMHMM-2.0/) was analyzed. Ure4 was presumed to contain 3 low-probability putative transmembrane domains which may interfere with the binding of Ure4 to Ure1. In order to identify and simultaneously map the putative interacting domain(s) of Ure4, 5 different deletion mutants with truncated versions of Ure4, each excluding either one or two of the transmembrane regions, were made. The truncated Ure4 containing amino acid residues 90 to 230 (Ure4aa90-230) was the only construct that interacted with Ure1 (Fig. 4A). Interestingly, when amino acid residues 90 to 230 were fused to the amino-terminal domain consisting of amino acid residues 1 to 89 (Ure4aa1-230) or carboxyl-terminal domain amino acid residues 231 to 327 (Ure4aa90-327), no interaction with Ure1 occurred. It can, therefore, be hypothesized that amino acid residues 90 to 230 of Ure4 interact with Ure1 whereas the presence of aa 1 to 89 and aa 231 to 327 interferes with Ure1 interaction. Alternatively, direct physiological interaction between Ure1 and Ure4 may be absent or too weak to be detected by the Y2H system and the observed interaction between Ure1 and Ure4aa90-230 could be an experimental artifact. Unlike Ure4, however, positive interaction occurred between Ure1 and full-length Ure6 and Ure7. Full-length Ure4 also interacted with both Ure6 and Ure7, and Ure6 in turn associated with Ure7. While all but Ure4aa1-57 interacted with Ure7, none of the truncated Ure4 mutants interacted with Ure6 (data not shown). An illustration summarizing the depicted Y2H interaction of Ure1 apoenzyme with the urease accessory proteins Ure4, Ure6, and Ure7 is presented in Fig. 4B.

The *URE2* gene is unrelated to urease function in *C. neoformans*. In the currently available annotated genomic sequence database of *C. neoformans*, we noticed the tight linkage (269 bp of separation) of the urease accessory protein gene *URE4* with *URE2* on chromosome 5 (see Fig. S2A in the supplemental material). We also found that the original DNA fragment from cryptococcal genomic library that had been used to complement the urease-negative phenotype of the clinical isolate (B-4587) contained both the *URE4* and *URE2* gene sequences. Although *URE2* had been proposed to complement the urease-negative phenotype of B-4587 (1), *URE2* is homologous to *SMC3*, the mitosis-associated gene, which is not known to be involved in urease function. We suspected that the *URE4* gene and not *URE2* was responsible for the complementation of the urease-negative phenotype in B-4587. To test this, we constructed new *ure2*Δ strains in the H99 background. A qualitative spot assay on Christensen's agar demonstrated that *ure2*Δ strains remained urease positive and turned agar media pink in a manner similar to that seen with their WT strains (data not shown). Furthermore, when these two gene sequences were separately cloned from the original complementing DNA fragment and used in the transformation of B-4587 ("ure2" strain), only the *URE4* and not the *URE2* sequence restored the

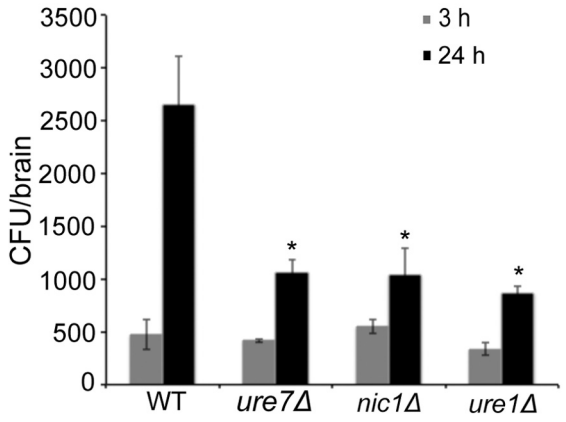

FIG 5 A functional urease system is involved in *C. neoformans* pathogenicity. Mutants lacking urease accessory proteins invade the brain less effectively than the parental strain. The results of determinations of brain CFU levels in C57BL/6 mice recovered 3 h (gray bar) and 24 h (black bar) after intravenous injection via the tail vein with 2×10^5 cells of *C. neoformans* are shown. Data represent means ± standard deviations (SD) ($n = 3$). *, $P < 0.01$ (compared to the WT strain).

urease phenotype (see Fig. S2B in the supplemental material). Therefore, *URE2* is not involved in urease function.

Mutants lacking a urease accessory protein or nickel transporter invade the brain less effectively than the parental strain. A urease-negative (*ure1*Δ) mutant has been reported to enter the mouse brain less effectively and is less virulent than the WT strain (18, 35). If urease activity and not the presence of the Ure1 protein itself were important for effective brain invasion, one would expect to find urease accessory gene mutants to also be less effective in mouse brain invasion than the WT strain. We compared the effectiveness of brain invasion by mutants of accessory proteins with WT. Colony forming units (CFU) levels in the brain of mice infected intravenously with mutants *ure7*Δ, *nic1*Δ, *ure1*Δ and the WT strain were determined at 3 and 24 h postinfection. There was no difference between the CFU in mice infected with different strains at 3 h. However, CFU levels at 24 h were significantly lower (<40%) in mice infected with all three mutants than in the WT-infected mice. The brain CFU levels of mice infected with each of the three urease-negative deletant strains were similar at 24 h (Fig. 5). To determine CFU levels that were representative of the urease-negative mutants, we compared the brain CFU values of the mice infected with *ure7*Δ and complemented strains and found that the *ure7*Δ strain complemented with the *URE7* gene restored the phenotype (see Fig. S3A in the supplemental material). The efficiency of brain invasion decreased significantly in mice infected with the *ure1* deletant strain as well as in those infected with the strains that contained *URE1* but had a deletion of one of the three accessory proteins, *viz.*, Ure7 or Nic1. This suggests the importance of urease activity and not of the presence of Ure1 protein in cryptococcal pathogenesis.

The integrity of the tight junction is affected by urease-positive *C. neoformans*. Since urease activity and not the Ure1 protein appeared to be important for brain invasion, we asked if the integrity of human BMECs (HBMECs) (blood-brain barrier [BBB]) is compromised under conditions of exposure to urease-positive *C. neoformans* cells. ZO-1 is one of the marker proteins used to test the integrity of the tight junctions of the endothelial cells. The protein is located on the cytoplasmic membrane surface of intercellular tight junctions (36). The integrity of the tight junction was not affected significantly by the 6 h of exposure to *C. neoformans* (data not shown). To determine if *C. neoformans* cells affected the integrity of HBMEC tight junctions at all, we prolonged the incubation period to 24 h. Due to the absence of a true positive control, a pathogenic *E. coli* strain E44 (5) which is known to be an effective disrupter of the tight junctions was used as the positive control. Degradation of ZO-1 by *E. coli* was apparent almost immediately (see Fig. S3B in the supplemental material). The protein blots showed that only the WT strain could partially reduce the amount of the ZO-1 proteins after 24 h of incubation (arrow). ZO-1 signals also decreased, although slightly, in the presence of *ure1*Δ+*URE1* in a time-dependent manner. On the other hand, the *ure1*Δ mutant had little or no detectable effect, even after 24 h of incubation. These data suggest that there is a detectable difference in the effect on ZO-1 stability between the HBMEC exposed to urease-positive strains and those exposed to urease-negative strains.

DISCUSSION

This is the first report that identifies and characterizes all the relevant genetic components and their biochemical functions required for the activation of the urease apoenzyme in a fungal species. The cryptococcal genome database shows the existence of a single urease gene identified so far that is homologous to those in most plants such as potato, tomato, and *Arabidopsis* sp. (37). Cryptococcal urease accessory genes are not clustered, unlike the bacterial urease accessory genes. In addition, the absence of a homologue of bacterial *ureE* in *C. neoformans* and its Ure7 carrying the dual roles of bacterial UreE and UreG suggests its greater resemblance to those of plants.

The accessory proteins in the cryptococcal urease system are homologous to those of the bacterial system except for UreE, the Ni divalent cation chaperone. Although an iron-containing urease has recently been reported in the bacterial pathogen *Helicobacter mustelae* (38, 39), urease in general is an exclusively nickel-dependent enzyme. The Ni chaperone function for the *C. neoformans* urease depends on the presence of a nickel-binding member of the GTPase family of proteins, Ure7. A mutant lacking Ure7 has no urease activity due to a lack of nickel incorporation into the enzyme. Analysis of nickel binding to Ure7 *in vitro* identified two nickel atoms binding with a K_d of less than 1 μM. A similar study of the bacterial UreG from *Klebsiella aerogenes* (Ka) established that this protein binds one equivalent of nickel with a K_d of 16 ± 3.1 μM (28). Excluding the histidine-rich amino-terminal domain, cryptococcal Ure7 and KaUreG share extensive (51%) amino acid identity. It is therefore possible that both proteins contain a conserved nickel binding site, which in *K. aerogenes* has been proposed to be involved in nickel transfer during urease maturation (28). In *C. neoformans*, the additional nickel atom in Ure7 is presumably bound via residues in the amino-terminal domain and may compensate for the lack of UreE—a bacterial nickel chaperone. In this model, Ure7 could have a dual function as a nickel chaperone and GTPase. The complete absence of the urease activity in the mutant carrying a His-to-Ala substitution within the second His-rich site (residues 80 to 82) in the amino-terminal end of Ure7 suggested that these His residues bind nickel. This second His-rich site is highly conserved among fungal homologs of UreG proteins. However, further work is required to

determine if the potential nickel chaperone function can be uncoupled from its role as a GTPase. The Ure7 and KaUreG proteins both generate a UV-visible light spectrum with a peak in the region of 330 nm that is consistent with a thiolate-to-nickel charge transfer (28). The KaUreG LMCT is dependent on the presence of a cysteine residue (Cys72) that is conserved in Ure7 (Cys173). However, it was noted in the KaUreG study that the results of the UV-visible light analysis were not consistent with those of the equilibrium dialysis experiments that established the stoichiometry of nickel binding. Similarly, we found that passage of the LMCT-generating form of Ure7 through a Sephadex G-25 column resulted in the loss of the 330-nm peaks but retention of approximately two atoms of nickel per Ure7 monomer (data not shown). Therefore, the two-nickel bound form of Ure7 does not give rise to a diagnostic LMCT that would indicate nickel being coordinated by a cysteine residue in Ure7.

The Y2H assays confirming the physical interaction of Ure1 apoprotein with all the accessory proteins and that all accessory protein mutants lack urease activity suggested that Ure1 formed a complex through interaction with its accessory proteins to become an active enzyme. However, protein instability could be a possible explanation for the failure to detect any association between the truncated Ure4aa1-57 and the accessory proteins. As in bacterial urease systems, there may be a sequential association of Ure1 with Ure4, Ure6, and Ure7 that leads to the activation of the cryptococcal urease enzyme. The details of such a sequential association in the cryptococcal urease system remain to be elucidated. Surprisingly, although urea supported the growth of the *Nic1*Δ mutant to a limited extent, this mutant could turn Christensen's agar pink in a delayed manner and changed the color of the agar after addition of external nickel into the media. These observations suggest the presence of some other low-affinity nickel transporter(s) in *Cryptococcus neoformans*. Additionally, the Nic1-dependent accumulation of nickel at very low levels suggests that Nic1 may be a nickel transporter but may not be the only one. However, our mouse studies performed with the *nic1*Δ mutant suggest that the mutants, which may accumulate very low levels of nickel through activity associated with other transporters or even other metals (such as cobalt), were avirulent, with a significant reduction in brain fungal loads. Thus, the nickel accumulation in the *nic1*Δ mutant, if there had been any, did not appear sufficient to indicate the presence of a functional urease. Interestingly, urease activity is regulated in response to the available nitrogen source, suggesting that this fungal regulatory mechanism ensures that the correct transporters and catabolic enzymes are expressed in response to the availability and type of nitrogen source present (40).

Urease in fungal pathogens may have a role to play in ensuring utilization of host urea as a nutrient. Urea is present in humans at millimolar concentrations, is able to pass across biological membranes, and is evenly distributed in the subcutaneous adipose tissue, central nervous system (CNS), epithelial lining fluid, and blood serum (41–44). In a mouse model of cryptococcosis, urease was reported to promote polarization of the immune system to a Th2 rather than the more effective Th1 response, possibly through pH-mediated changes to the adaptive immune system (45). Urease also appeared to enhance transmigration of *C. neoformans* across the BBB, resulting possibly from toxic effects of urea-derived ammonia on the endothelial cells of brain capillaries (35). Our analysis performed with the *in vitro* BBB model showed little effect of the *ure1*Δ strain on the integrity of the HBMEC, judging by the lack of changes in the levels of the junction protein ZO1. In contrast, the urease-positive WT strain caused a reduction in the ZO1 protein levels by 24 h, supporting earlier reports which have also suggested that cryptococcal urease compromises the integrity of the BBB. When a urease inhibitor was administered to mice infected with the wild-type *C. neoformans*, fungal dissemination to the brain was significantly reduced, most probably due to reduction in the sites of transmigration (35). Earlier reports on histological analysis of the cryptococcal blood-to-brain invasion (46–48) showed wedging of the yeasts in small capillaries, structural alteration of microvessel walls, and formation of mucoid cysts initiated in the proximity of damaged microcapillaries (18). Cryptococcal urease has also been shown to contribute to CNS invasion by enhancing yeast sequestration within microcapillary beds in brain during hematogenous spread (35). Our study showed no difference in the brain fungal load between WT and urease-negative strains at 3 h postinfection (via tail vein) but showed a significant difference by 24 h, supporting the idea that urease affects transmigration of yeasts into the brain parenchyma. The trapping of the yeast in microvessels could occur due to its physical size (49) and/or biological force (50), e.g., in the interaction between cryptococcal hyaluronic acid and host CD44. Since urease activity is important for brain invasion, characterization of the urease activation system is vital for our understanding of cryptococcal clinicopathology and of that of other urease-positive pathogens that cause brain infection.

MATERIALS AND METHODS

Ethics statement. The animal studies conducted were in full compliance with all of the guidelines set forth by the Institutional Animal Care and Use Committee (IACUC) of the National Institute of Allergy and Infectious Diseases, National Institutes of Health, and were in full compliance with the United States Animal Welfare Act (Public Law 98-198). The NIAID IACUC (permit no. LCID50E) approved all of the vertebrate studies which were conducted in facilities accredited by the Association for Assessment and Accreditation of Laboratory Animal Care (AAALAC).

Strains and media. The strains included *C. neoformans* H99 and its genetically manipulated derivative strains: mutants *ure1*Δ, *ure4*Δ, *ure6*Δ, *ure7*Δ, *nic1*Δ, and *ure2*Δ. The reconstituted strains *ure1*Δ+*URE1*, *ure4*Δ+*URE4*, *ure6*Δ+*URE6*, *ure7*Δ+*URE7*, *nic1*Δ+*NIC1*, and *ure2*Δ+*URE2* were all derived from the respective deletant strains. Y2H Gold (*MAT*a) and Y187 (*MAT*α) are derivative strains of *S. cerevisiae*. *C. neoformans* cultures were grown in YPD (2% glucose, 1% yeast extract, 2% peptone) medium or YNB (1.7 g liter^{-1} yeast nitrogen base, 2% glucose) medium with ammonium sulfate (5 g liter^{-1}), urea (2.27 g liter^{-1}), proline (8.7 g liter^{-1}), glutamine (5.53 g liter^{-1}), or glutamic acid (12.78 g liter^{-1}) as a nitrogen source. Christensen's urea agar medium (catalog no. 27048; Sigma) was used for phenotypic assays of urease activity. Strains *ure1*Δ and *ure1*Δ+*URE1* were obtained from John R. Perfect.

mRNA analysis by S1 nuclease. Total RNA was isolated from a mid-log-phase culture and was hybridized with ^{32}P-labeled, single-stranded DNA oligonucleotides that were complementary to the *URE1* and *CMD1* (control) genes. Following digestion with S1 nuclease, the samples were electrophoresed through an 8% polyacrylamide and 5 M urea gel.

Gene deletions. The urease accessory genes *URE4* (CNAG_01166), *URE6* (CNAG_02057), *URE7* (CNAG_00678), the presumed nickel transporter *NIC1* (CNAG_03664), and *URE2* (CNAG_01167) identified from the H99 genome database (http://www.broadinstitute.org/annotation/genome/cryptococcus_neoformans/MultiHome.html) were all deleted from H99. Disruption constructs (see Table S1 in the supplemental material for a list of primers) were created by an overlapping PCR

technique (51) or by vector cloning linked with G418 (*NEO*) resistance genes as dominant selectable markers. The resulting constructs were transformed into the H99 cells as previously described (52). Transformants with deletion of the correct locus were confirmed by PCR and Southern blot analysis.

Cloning of the target genes and complementation of their respective deletion strains. The DNA sequences of *URE4*, *URE6*, *URE7*, *NIC1*, and *URE2* were amplified by PCR using platinum Hi-Fi DNA polymerase enzyme (Invitrogen). Oligonucleotide primers were designed to amplify at least 500 bp flanking the coding region of each respective gene, and the amplified sequences were then ligated into *E. coli* plasmid vector TOPO (Invitrogen) that had been modified to contain the *NAT* or *HYG* gene. The plasmids containing the cloned genes were transformed into the respective deletant strains. Drug-resistant colonies were tested for urease activity and growth on Christensen's medium and urea media, respectively.

Protein extraction. Protein was extracted from each cryptococcal strain using a method described previously (53). Briefly, 10 ml of a mid-log-phase culture was pelleted, washed twice in cold water, and snap-frozen in liquid nitrogen. The pellet was thawed on ice and resuspended in extraction buffer (40 mM Tris-HCl, 20 mM dithiothreitol [DTT], 4% Triton X-100, 1 mM EDTA, 2 mM phenylmethylsulfonyl fluoride [PMSF], protease inhibitor cocktail, pH 9). An equal volume of glass beads (0.5 μm) was added to rupture the cells using a BeadBeater (20 s of processing followed by 2 min on ice for 6 cycles), the reaction mixture was centrifuged (10,000 $\times$ *g*, 10 min, 4°C), and the protein concentration in the supernatant was assayed with Bradford reagent.

Urease activity assays. Protein extracts from each strain (100 μg) were added to 1.0 ml of urea solution (66 mM) in reaction buffer (10 mM potassium phosphate, 10 mM lithium chloride, 1 mM EDTA, pH 8.2), mixed well, and incubated at 30°C. A 150-μl volume was removed from the reaction mixture at 0, 10, 20, 30, and 40 min and added to 750 μl Nessler's color reagent (20% Nessler's reagent [catalog no. 345148; Sigma], 0.08% Ficoll). Absorbance (480 nm) was measured and used to calculate ammonia production over time. Units of urease represent the liberation of 1 μmol ammonia per min (pH 8.2, 30°C).

Metal accumulation assays. Aliquots (10 ml) of a mid-log-phase culture were pelleted, washed twice, snap-frozen in liquid nitrogen, and thawed at room temperature, and 1 ml of Suprapure nitric acid (65%) (VWR) was added. The samples were incubated at room temperature for 3 days with occasional vortexing to dissolve all cellular material. The acid-digested samples were then centrifuged (3,000 rpm, 30 min) to remove insoluble particles, diluted 5-fold in dilute nitric acid (2%) containing 20 μg liter^{-1} Ag as an internal standard, and analyzed by ICP-MS (Thermo X-Series) using the peak jump method in standard operating mode, monitoring ^{60}NI, ^{59}Co, and ^{117}Ag (30 ms dwell time each on 5 channels with separation at 0.02 atomic mass units [AMU] for 100 reads, in triplicate), and concentrations were determined by comparison to matrix-matched elemental standards.

Metal profiles. Metal profile analyses were performed as previously described (21). A mid-log-phase *C. neoformans* culture (1 liter) was pelleted, washed, and snap-frozen in liquid nitrogen. The pellet was thawed in HEPES buffer (50 mM, pH 8), and the cells were lysed by grinding with mortar and pestle under liquid nitrogen. The disrupted cells were thawed under anaerobic conditions (<2 ppm O_2) in an N_2 atmosphere glove box (Belle Technologies, United Kingdom) and unbroken cells and membranes removed by centrifugation (8,000 rpm, 15 min) and ultracentrifugation (30,000 rpm, 30 min), respectively. Protein extract (30 mg) was loaded onto a 1 ml Hi-Trap Q FF anion exchange column (GE Healthcare) and sequentially eluted in 3 volumes of 1 ml buffer (50 mM Tris, pH 8.8) containing 100 mM, 200 mM, and 300 mM of NaCl, respectively. Aliquots of the 300 mM fraction (200 μl) were subjected to size exclusion HPLC on a TSK-SW3000 column (Tosoh Biosciences) in HPLC buffer (10 mM Tris, 50 mM NaCl, pH 7.5). Urease activity was determined as described above by addition of an aliquot (5 μl) of HPLC fractions to a urea solution (45 μl, 66 mM) in urease reaction buffer with incubation at 30°C for 40 min followed by addition of Nessler's color reagent (200 μl). Metal content was quantified by ICP-MS after 10-fold dilution of each fraction in nitric acid (2.5%) containing 20 μg liter^{-1} Ag as an internal standard.

Purification of Ure7 protein. Recombinant Ure7 was expressed in *E. coli* strain BL21 containing plasmid pET29a-Ure7, which was generated by amplifying Ure7 cDNA from the H99 mRNA and ligating the resulting product into the NdeI site of pET29a. Correct amplification and cloning were confirmed by sequencing. *E. coli* cultures containing pET29a-Ure7 were grown at 37°C to an optical density at 600 nm (OD_{600}) of 0.6, the cultures were moved to 30°C, $NiSO_4$ was added (1 mM), and Ure7 expression was induced by addition of isopropyl-β-D-thiogalactopyranoside (IPTG) (1 mM). The addition of $NiSO_4$ increased the solubility of overexpressed Ure7. After 6 h of induction, the cells were harvested by centrifugation and frozen. The cells were resuspended in binding buffer (50 mM Tris-HCl, 300 mM NaCl, pH 8) with 10 mM imidazole and subjected to lysis by the use of a French press (3 passages at 25,000 lb/in^2). The crude extract was centrifuged (30,000 rpm, 20 min) to remove insoluble cell debris and then loaded onto a 5 ml His-trap column (GE) followed by washing with 4 column volumes of binding buffer. Ure7 was eluted using a linear gradient of imidazole (10 mM to 300 mM) over 20 column volumes. Fractions containing Ure7 were pooled and diluted (10-fold) in binding buffer before reloading onto the His-Trap column was performed. A second elution step used a linear gradient of imidazole (60 mM to 200 mM) over 80 column volumes. Fractions containing purified Ure7 were pooled, diluted (5-fold), and then concentrated by reloading onto the His-Trap column and eluted with imidazole (300 mM) in a single step. Any metal bound to Ure7 was removed by incubation with EDTA (1 mM) for ~72 h (4°C). Imidazole, EDTA, and NaCl were removed by serial buffer exchanges into Tris-HCl (20 mM, pH 8) using a Centricon centrifugal filter (Millipore).

Analysis of Ure7 metal binding. A solution of Ure7 protein (3 μM) was incubated with 20 M equivalents of Ni or Co at 4°C, the Ure7-metal mixture was loaded onto a Sephadex G-25 desalting column (GE), and 1-ml fractions were eluted. The metal content and protein concentration of the eluted fractions were analyzed by ICP-MS and a Bradford assay, respectively. To confirm the stoichiometry of metal binding to Ure7 by equilibrium dialysis, aliquots (500 μl) of Ure7 (3 μM) were dialyzed against 500 ml of Tris-HCl (10 mM, pH 8) with various concentrations of Ni or Co for 72 h. Metal concentrations in the sample and assay volumes were determined by ICP-MS and used to calculate the concentration of Ure7-associated metal. The dissociation constant, K_d, and binding capacity, B_{max}, were determined using a Hill plot (Origin software).

Genetic manipulation of Ure7 His-rich sites. Two highly conserved, N-terminal, histidine-rich sites of Ure7 (CNAG_00678) in H99 were selected for targeted mutation. These histidines were replaced by alanines to construct a series of Ure7 His residue mutant strains. Briefly, three fragments of sizes 1,200 bp, 130 bp, and 830 bp were amplified by PCR from H99 genomic DNA (see the list of primers in Table S1 in the supplemental material). The 130-bp fragment had either of two His-rich sites at each end, and primers to amplify this fragment were designed to replace histidine with alanine by changing nucleotide sequences from 115 to 123 or from 238 to 246 of the *URE7* open reading frame and to include specific sequences recognized by the restriction enzymes. Finally, 2.16 kb of DNA sequence composed of 1,200-bp, 130-bp, and 830-bp fragments was amplified by overlapping PCR and subcloned into pCR-BluntII-TOPO to construct pU7H1-1 (no mutation), pU7H2-1 (mutation at amino acid residues 39 to 41), pU7H3-1 (mutation at amino acid residues 80 to 82), and pU7H4-1 (mutation at amino acid residues 39 to 41 and 80 to 82). A 2.7-kb fragment composed of a 1.0-kb fragment upstream of *URE7* and a 1.7-kb fragment consisting of a *NAT* marker was subcloned into pCR-BluntII-TOPO to construct plasmid pU7H5. The 2.2-kb fragments from each of plasmids pU7H1-1, pU7H2-1, pU7H3-1, and pU7H4-1 and a 2.7-kb fragment from pU7H5 were restriction digested with ApaI and

XbaI and with BamHI and ApaI, respectively. These BamHI-ApaI and ApaI-XbaI fragments were ligated into the BamHI-XbaI site of vector pYCC884 to yield plasmids pU7H1-2, pU7H2-2, pU7H3-2, and pU7H4-2 using T4 DNA ligase (New England Biolabs). The final 4.9-kb fragments were restriction digested with BamHI and XbaI to get templates for homologous recombination in H99. Mutations on either of the His sites on Ure7 were verified by PCR amplification followed by restriction digestion and sequencing. The H99 strain was biolistically transformed with each fragment to generate strains *ure7H1*, *ure7H2*, *ure7H3*, and *ure7H4*. Homologous recombination was confirmed by PCR and by Southern hybridization (data not shown).

Yeast two-hybrid assay. cDNAs were raised for the full-length *URE1* (CNAG_05540), *URE4*, *URE6*, and *URE7* sequences and for the truncated versions of Ure4, *viz.*, aa 1 to 57, aa 90 to 230, aa 260 to 327, aa 1 to 230, and aa 90 to 327, with SuperScript III first-strand synthesis using either total RNA or the gene-specific primers according to the manufacturer's protocol. The list of primers used is given in Table S1 in the supplemental material. The full-length Ure1, Ure4, Ure6, and Ure7 and the truncated Ure4 (aa 1 to 57, aa 90 to 230, aa 260 to 327, aa 1 to 230, and aa 90 to 327) were first cloned in Topo-4.2 vector and then subcloned in frame in pGBK T7, the bait vector, and pGADT7, the prey vector of the Match-Maker gold yeast-two hybrid system (Clontech). The correct in-frame cloning of the required gene in the bait and prey vectors was confirmed by sequence analysis before proceeding. Analyses of the interaction between the target proteins were carried out by yeast mating and performed according to the manufacturer's protocol with little modification. In brief, concentrated cultures of both bait and prey proteins in the Y2H Gold and Y187 strains, respectively, were grown overnight, mixed, and mated for 24 h before being plated on double-drop-out (without tryptophan and leucine) and QDO (without tryptophan, leucine, adenine, and histidine and with or without aureobasidin A and X-α-Gal) selective-medium agar plates for screening of positive clones.

Virulence studies in mice. Animal studies were performed using 7-week-old female C57BL/6 mice. Brain fungal burdens were determined following intravenous injection of 2×10^5 cells or 5×10^4 cells per mouse via tail vein. Each mouse received 200 μl of cells suspended in saline solution, and the inoculum size was confirmed by CFU formed on YPD agar plate. The brains of mice (3 mice/strain) were isolated after 3 and 24 h postinjection, and CFUs were analyzed (46).

Western blots. HBMECs were grown in a 10-cm-diameter dish until confluence and were then treated with different *C. neoformans* strains (10^6 cells). The treated cultures were harvested at 0.1 (immediately), 16, and 24 h and then washed three times with phosphate-buffered saline and lysed with protein loading buffer. Equal volumes were used for all samples. β-Actin was used as the loading control. The blots were probed with anti-ZO1 antibodies (catalog no. 443200; Genescript, Inc.).

Statistical analysis. An unpaired *t* test was used for the statistical analysis. A *P* value of less than 0.05 was considered statistically significant.

SUPPLEMENTAL MATERIAL

Supplemental material for this article may be found at http://mbio.asm.org/lookup/suppl/doi:10.1128/mBio.00220-13/-/DCSupplemental.

Figure S1, TIF file, 13 MB.
Figure S2, TIF file, 7.8 MB.
Figure S3, TIF file, 5.4 MB.
Table S1, DOCX file, 0.1 MB.

ACKNOWLEDGMENTS

We thank Samantha Dainty for her early technical contribution to this work.

This study was supported by the Intramural Research Program of the U.S. National Institute of Allergy and Infectious Diseases, National Institutes of Health (K.J.K.-C.), and by the Research Councils United Kingdom Academic Fellowship and Marie Curie International Re-Integration Grant to J.C.R. R.J.P. was supported by a Biotechnology and Biological Sciences Research Council studentship. Funding from the Royal Society (RG100365) and from Newcastle University Faculty of Medical Sciences supported K.J.W. The funders had no role in study design, data collection and analysis, decision to publish, or preparation of the manuscript.

REFERENCES

1. **Varma A, Wu S, Guo N, Liao W, Lu G, Li A, Hu Y, Bulmer G, Kwon-Chung KJ.** 2006. Identification of a novel gene, URE2, that functionally complements a urease-negative clinical strain of *Cryptococcus neoformans*. Microbiology **152**:3723–3731.DOI:10.1099/mic.0.2006/000133-0
2. **Cox GM, Mukherjee J, Cole GT, Casadevall A, Perfect JR.** 2000. Urease as a virulence factor in experimental cryptococcosis. Infect. Immun. **68**:443–448.DOI:10.1128/IAI.68.2.443-448.2000
3. **Mirbod-Donovan F, Schaller R, Hung CY, Xue J, Reichard U, Cole GT.** 2006. Urease produced by *coccidioides posadasii* contributes to the virulence of this respiratory pathogen. Infect. Immun. **74**:504–515.DOI:10.1128/IAI.74.1.504-515.2006
4. **Rappleye CA, Goldman WE.** 2006. Defining virulence genes in the dimorphic fungi. Annu. Rev. Microbiol. **60**:281–303.DOI:10.1146/annurev.micro.59.030804.121055
5. **Mobley HL, Island MD, Hausinger RP.** 1995. Molecular biology of microbial ureases. Microbiol. Rev. **59**:451–480.
6. **Torisky RS, Polacco JC.** 1990. Soybean roots retain the seed urease isozyme synthesized during embryo development. Plant Physiol. **94**:681–689.DOI:10.1104/pp.94.2.681
7. **Witte CP, Isidore E, Tiller SA, Davies HV, Taylor MA.** 2001. Functional characterisation of urease accessory protein G (ureG) from potato. Plant Mol. Biol. **45**:169–179.DOI:10.1023/A:1006429315851
8. **Witte CP, Medina-Escobar N.** 2001. In-gel detection of urease with nitroblue tetrazolium and quantification of the enzyme from different crop plants using the indophenol reaction. Anal. Biochem. **290**:102–107.DOI:10.1006/abio.2000.4933
9. **Strope PK, Nickerson KW, Harris SD, Moriyama EN.** 2011. Molecular evolution of urea amidolyase and urea carboxylase in fungi. BMC Evol. Biol. **11**:.DOI:10.1186/1471-2148-11-8080.
10. **Bacanamwo M, Witte CP, Lubbers MW, Polacco JC.** 2002. Activation of the urease of *Schizosaccharomyces pombe* by the UreF accessory protein from soybean. Mol. Genet. Genomics **268**:525–534.DOI:10.1007/s00438-002-0769-z
11. **Yu JJ, Smithson SL, Thomas PW, Kirkland TN, Cole GT.** 1997. Isolation and characterization of the urease gene (URE) from the pathogenic fungus *coccidioides immitis*. Gene **198**:387–391.DOI:10.1016/S0378-1119(97)00342-9
12. **Sumner JB.** 1926. The isolation and characterization of the enzyme urease. J. Biol. Chem. **69**:435–441.
13. **Jabri E, Carr MB, Hausinger RP, Karplus PA.** 1995. The crystal structure of urease from *Klebsiella aerogenes*. Science **268**:998–1004.DOI:10.1126/science.7754395
14. **Moncrief MB, Hausinger RP.** 1997. Characterization of UreG, identification of a UreD-UreF-UreG complex, and evidence suggesting that a nucleotide-binding site in UreG is required for in vivo metallocenter assembly of *Klebsiella aerogenes* urease. J. Bacteriol. **179**:4081–4086.
15. **Lee MH, Mulrooney SB, Renner MJ, Markowicz Y, Hausinger RP.** 1992. Klebsiella aerogenes urease gene cluster: sequence of ureD and demonstration that four accessory genes (ureD, ureE, ureF, and ureG) are involved in nickel metallocenter biosynthesis. J. Bacteriol. **174**:4324–4330.
16. **Mulrooney SB, Hausinger RP.** 1990. Sequence of the *Klebsiella aerogenes* urease genes and evidence for accessory proteins facilitating nickel incorporation. J. Bacteriol. **172**:5837–5843.
17. **Follmer C.** 2008. Insights into the role and structure of plant ureases. Phytochemistry **69**:18–28.DOI:10.1016/j.phytochem.2007.06.034
18. **Olszewski MA, Noverr MC, Chen GH, Toews GB, Cox GM, Perfect JR, Huffnagle GB.** 2004. Urease expression by *Cryptococcus neoformans* promotes microvascular sequestration, thereby enhancing central nervous system invasion. Am. J. Pathol. **164**:1761–1771.DOI:10.1016/S0002-9440(10)63734-0
19. **Peterson CL.** 1994. The SMC family: novel motor proteins for chromosome condensation? Cell **79**:389–392.DOI:10.1016/0092-8674(94)90247-X
20. **Holt CL, May GS.** 1996. An extragenic suppressor of the mitosis-defective bimD6 mutation of *Aspergillus nidulans* codes for a chromosome scaffold protein. Genetics **142**:777–787.

21. **Tottey S, Waldron KJ, Firbank SJ, Reale B, Bessant C, Sato K, Cheek TR, Gray J, Banfield MJ, Dennison C, Robinson NJ.** 2008. Protein-folding location can regulate manganese-binding versus copper- or zinc-binding. Nature **455**:1138–1142.DOI:10.1038/nature07340
22. **Yang M, Cobine PA, Molik S, Naranuntarat A, Lill R, Winge DR, Culotta VC.** 2006. The effects of mitochondrial iron homeostasis on cofactor specificity of superoxide dismutase 2. EMBO J. **25**:1775–1783.DOI:10.1038/sj.emboj.7601064
23. **Howard DH.** 1999. Acquisition, transport, and storage of iron by pathogenic fungi. Clin. Microbiol. Rev. **12**:394–404.
24. **Nishimura K, Igarashi K, Kakinuma Y.** 1998. Proton gradient-driven nickel uptake by vacuolar membrane vesicles of *Saccharomyces cerevisiae*. J. Bacteriol. **180**:1962–1964.
25. **Park IS, Hausinger RP.** 1993. Site-directed mutagenesis of *Klebsiella aerogenes* urease: identification of histidine residues that appear to function in nickel ligation, substrate binding, and catalysis. Protein Sci. **2**:1034–1041.DOI:10.1002/pro.5560020616
26. **Song HK, Mulrooney SB, Huber R, Hausinger RP.** 2001. Crystal structure of *Klebsiella aerogenes* UreE, a nickel-binding metallochaperone for urease activation. J. Biol. Chem. **276**:49359–49364.DOI:10.1074/jbc.M108619200
27. **Webster J, Oxley D.** 2005. Peptide mass fingerprinting: protein identification using MALDI-TOF mass spectrometry. Methods Mol. Biol. **310**:227–240.DOI:10.1007/978-1-59259-948-6_16
28. **Boer JL, Quiroz-Valenzuela S, Anderson KL, Hausinger RP.** 2010. Mutagenesis of *Klebsiella aerogenes* UreG to probe nickel binding and interactions with other urease-related proteins. Biochemistry **49**:5859–5869.DOI:10.1021/bi1004987
29. **Eitinger T, Degen O, Bohnke U, Muller M.** 2000. Nic1p, a relative of bacterial transition metal permeases in *Schizosaccharomyces pombe*, provides nickel ion for urease biosynthesis. J. Biol. Chem. **275**:18029–18033.DOI:10.1074/jbc.M001978200
30. **Eitinger T, Friedrich B.** 1991. Cloning, nucleotide sequence, and heterologous expression of a high-affinity nickel transport gene from *Alcaligenes eutrophus*. J. Biol. Chem. **266**:3222–3227.
31. **Eitinger T, Wolfram L, Degen O, Anthon C.** 1997. A Ni2+ binding motif is the basis of high affinity transport of the *Alcaligenes eutrophus* nickel permease. J. Biol. Chem. **272**:17139–17144.DOI:10.1074/jbc.272.27.17139
32. **Degen O, Eitinger T.** 2002. Substrate specificity of nickel/cobalt permeases: insights from mutants altered in transmembrane domains I and II. J. Bacteriol. **184**:3569–3577.DOI:10.1128/JB.184.13.3569-3577.2002
33. **Fields S, Song O.** 1989. A novel genetic system to detect protein-protein interactions. Nature **340**:245–246.DOI:10.1038/340245a0
34. **Yu Z, Feng D, Liang C.** 2004. Pairwise interactions of the six human MCM protein subunits. J. Mol. Biol. **340**:1197–1206.DOI:10.1016/j.jmb.2004.05.024
35. **Shi M, Li SS, Zheng C, Jones GJ, Kim KS, Zhou H, Kubes P, Mody CH.** 2010. Real-time imaging of trapping and urease-dependent transmigration of *Cryptococcus neoformans* in mouse brain. J. Clin. Invest. **120**:1683–1693.DOI:10.1172/JCI41963
36. **Anderson JM, Stevenson BR, Jesaitis LA, Goodenough DA, Mooseker MS.** 1988. Characterization of ZO-1, a protein component of the tight junction from mouse liver and Madin-Darby canine kidney cells. J. Cell Biol. **106**:1141–1149.DOI:10.1083/jcb.106.4.1141
37. **Witte CP, Rosso MG, Romeis T.** 2005. Identification of three urease accessory proteins that are required for urease activation in *Arabidopsis*. Plant Physiol. **139**:1155–1162.DOI:10.1104/pp.105.070292
38. **Carter EL, Tronrud DE, Taber SR, Karplus PA, Hausinger RP.** 2011. Iron-containing urease in a pathogenic bacterium. Proc. Natl. Acad. Sci. U. S. A. **108**:13095–13099.DOI:10.1073/pnas.1106915108
39. **Stoof J, Breijer S, Pot RG, van der Neut D, Kuipers EJ, Kusters JG, van Vliet AH.** 2008. Inverse nickel-responsive regulation of two urease enzymes in the gastric pathogen *Helicobacter mustelae*. Environ. Microbiol. **10**:2586–2597.DOI:10.1111/j.1462-2920.2008.01681.x
40. **Marzluf GA.** 1997. Genetic regulation of nitrogen metabolism in the fungi. Microbiol. Mol. Biol. Rev. **61**:17–32.
41. **Ronne-Engström E, Cesarini KG, Enblad P, Hesselager G, Marklund N, Nilsson P, Salci K, Persson L, Hillered L.** 2001. Intracerebral microdialysis in neurointensive care: the use of urea as an endogenous reference compound. J. Neurosurg. **94**:397–402.DOI:10.3171/jns.2001.94.3.0397
42. **Tyvold SS, Solligård E, Lyng O, Steinshamn SL, Gunnes S, Aadahl P.** 2007. Continuous monitoring of the bronchial epithelial lining fluid by microdialysis. Respir. Res. **8**:.DOI:10.1186/1465-9921-8-7878.
43. **Waring WS, Stephen AF, Robinson OD, Dow MA, Pettie JM.** 2008. Serum urea concentration and the risk of hepatotoxicity after paracetamol overdose. QJM **101**:359–363.DOI:10.1093/qjmed/hcn023
44. **Zielinski H, Mudway IS, Bérubé KA, Murphy S, Richards R, Kelly FJ.** 1999. Modeling the interactions of particulates with epithelial lining fluid antioxidants. Am. J. Physiol. **277**:L719–L726.
45. **Osterholzer JJ, Surana R, Milam JE, Montano GT, Chen GH, Sonstein J, Curtis JL, Huffnagle GB, Toews GB, Olszewski MA.** 2009. Cryptococcal urease promotes the accumulation of immature dendritic cells and a non-protective T2 immune response within the lung. Am. J. Pathol. **174**:932–943.DOI:10.2353/ajpath.2009.080673
46. **Chang YC, Stins MF, McCaffery MJ, Miller GF, Pare DR, Dam T, Paul-Satyaseela M, Kim KS, Kwon-Chung KJ, Paul-Satyasee M.** 2004. Cryptococcal yeast cells invade the central nervous system via transcellular penetration of the blood-brain barrier. Infect. Immun. **72**:4985–4995.DOI:10.1128/IAI.72.9.4985-4995.2004
47. **Charlier C, Nielsen K, Daou S, Brigitte M, Chretien F, Dromer F.** 2009. Evidence of a role for monocytes in dissemination and brain invasion by *Cryptococcus neoformans*. Infect. Immun. **77**:120–127.DOI:10.1128/IAI.01065-08
48. **Eisenman HC, Casadevall A, McClelland EE.** 2007. New insights on the pathogenesis of invasive *Cryptococcus neoformans* infection. Curr. Infect. Dis. Rep. **9**:457–464.DOI:10.1007/s11908-007-0070-8
49. **Jong A, Wu CH, Shackleford GM, Kwon-Chung KJ, Chang YC, Chen HM, Ouyang Y, Huang SH.** 2008. Involvement of human CD44 during *Cryptococcus neoformans* infection of brain microvascular endothelial cells. Cell. Microbiol. **10**:1313–1326.DOI:10.1111/j.1462-5822.2008.01128.x
50. **Jong A, Wu CH, Gonzales-Gomez I, Kwon-Chung KJ, Chang YC, Tseng HK, Cho WL, Huang SH.** 2012. Hyaluronic acid receptor CD44 deficiency is associated with decreased *Cryptococcus neoformans* brain infection. J. Biol. Chem. **287**:15298–15306.DOI:10.1074/jbc.M112.353375
51. **Davidson RC, Blankenship JR, Kraus PR, de Jesus Berrios M, Hull CM, D'Souza C, Wang P, Heitman J.** 2002. A PCR-based strategy to generate integrative targeting alleles with large regions of homology. Microbiology **148**:2607–2615.
52. **Toffaletti DL, Rude TH, Johnston SA, Durack DT, Perfect JR.** 1993. Gene transfer in *Cryptococcus neoformans* by use of biolistic delivery of DNA. J. Bacteriol. **175**:1405–1411.
53. **Chai HC, Tay ST.** 2009. Detection of IgM and IgG antibodies to *Cryptococcus neoformans* proteins in blood donors and HIV patients with active cryptococcosis. Mycoses **52**:166–170.DOI:10.1111/j.1439-0507.2008.01549.x